



Travelling Ionospheric Disturbances Forecasting System

T-FORS

**Report on the definition of MSTID forecasting methodology
and data inventory**

Version 2.0



The T-FORS project has received funding from the European Union's Horizon Europe Research and Innovation Actions programme under Grant agreement No 101081835



Contents

Document Information.....	4
Document history.....	4
Disclaimer.....	5
Executive Summary.....	5
1. Purpose and Scope of the Document.....	6
2. Objectives of the MSTID climatology and probabilistic forecasting.....	7
3. General approach.....	8
3.1. Data Analysis.....	8
3.2. Methodologies.....	9
3.2.1 GNSS-TEC data.....	9
3.2.2 Ionosonde data.....	12
3.2.3 CDSS data.....	14
3.2.4 Airglow imager data.....	15
3.2.5 Swarm satellite data.....	16
3.2.6 Northern Annular Mode (NAM) data.....	17
4. Compilation of list of dynamic events.....	17
References.....	18

Document Information

Title:	Report on the definition of the MSTID forecasting methodology and data inventory
Date of Delivery:	09-June-23
Author(s):	Sivkandan Mani, Jens Mielich, Tobias Verhulst, Dalia Burešová, Veronika Barta, Anna Belehaki, David Altadill, Toni Seggarra, Dan Kouba, and Kitty A. Berényi
Work Package no.:	3
Work Package title:	MSTID climatology and probabilistic forecasting
Work Package leader:	IAP-L
Dissemination level:	Public
Nature:	Report

Document history

Version	Date	Edited by	Reason for modification / Remarks
1.0	08/06/2023	Sivkandan Mani, Jens Mielich, ...	First draft
2.0	12/06/2023	Sivkandan Mani, Jens Mielich, Tobias Verhulst, Dalia Burešová, Veronika Barta, Anna Belehaki, David Altadill, Toni Seggarra, Dan Kouba, and Kitty A. Berényi	Consolidated version

Disclaimer

This document contains description of the T-FORS project findings, work and products. Certain parts of it might be under partner Intellectual Property Right (IPR) rules so, prior to using its content please contact the Project Coordinator (Dr Anna Belehaki, belehaki@noa.gr) for approval.

In case you believe that this document harms in any way IPR held by you as a person or as a representative of an entity, please do notify us immediately.

The authors of this document have taken all reasonable measures in order for its content to be accurate, consistent and lawful. However, neither the project consortium as a whole nor the individual partners that implicitly or explicitly participated in the creation and publication of this document hold any sort of responsibility that might occur because of using its content by third parties.

This publication has been produced with the assistance of the European Union. The content of this publication is the sole responsibility of the T-FORS consortium and can in no way be taken to reflect the views of the European Union.

Executive Summary

T-FORS project aims at providing new models able to interpret a broad range of observations of the solar corona, the interplanetary medium, the magnetosphere, the ionosphere and the atmosphere, and to issue forecasts and warnings for TIDs several hours ahead [AD-1]. T-FORS expect to develop prototype services based on specifications from the users' community with a comprehensive architectural concept allowing for possible future adjustments in order to develop a real-time operational service. This document is a report for the definition of the MSTID forecasting models.

1. Purpose and Scope of the Document

This document presents the strategy for the establishment of the climatology of Medium Scale Traveling Ionospheric Disturbances characteristics such as occurrence, propagation direction, diurnal, seasonal and solar dependency, wavelength, phase speed and period, and using these information developments of a probabilistic forecasting over the European sector. The document is divided into four sections:

Section 1 (this section) describes the organisation of the document

Section 2 describes the objectives of the MSTIDs climatology and probabilistic forecasting.

Section 3 presents the approach of the data collection, data analysis and methodology applied for each data set and preliminary results of MSTIDs climatology.

Section 4 presents compilation of list of sporadic events that triggered MSTIDs.

Applicable Documents

The following table contains the list of applicable documents.

AD	Document title
[AD-1]	Grant Agreement number: 101081835 — T-FORS — HORIZON-CL4-2022-SPACE-01

Acronyms

The following table contains the list of all acronyms used in this document.

Table 1. List of acronyms

Acronym	Definition
2D	2-Dimension
BGD	Borealis Global Designs EOOD
CDSS	Continuous Doppler Sounding System
DPS-4D	Digisonde Portable Sounder model
dTEC	detrended TEC
Es	Sporadic-E
EW	East-West
EWK	EW Keogram
FFT	Fast Fourier Transform
FI	Foldfizikai es Urtudományi Kutatóintézet

Acronym	Definition
GFP	Bundespolizei
GNSS	Global Navigation Satellite System
IAP-L	Leibniz-Institut für Atmosphärenphysik ev an der Universität Rostock
IAP-P	Ustav Fyziky Atmosfery av CR, v.v.i.
INGV	Istituto Nazionale di Geofisica e Vulcanologia
LEO	Low-Earth-Orbiting
LSTID	Large Scale TID
MSTID	Medium Scale TID
NAM	Northern Annular Mode
NAO	North Atlantic/Arctic Oscillations
NOA	Ethniko Asteroskopeio Athinon (National Observatory of Athens)
NS	North-South
NSK	NS Keogram
OE	Observatorio del Ebro Fundación
ONERA	Office National d'Etudes et de Recherches Aeronautiques
RMI	Institut Royal Meteorologique de Belgique
TEC	Total Electron Content
TECU	TEC Unit
WP	Work-package

2. Objectives of the MSTID climatology and probabilistic forecasting

The main objective is to develop an empirical model of the MSTID occurrence based on the observational climatology over European sector. This empirical model will be also used to forecast the MSTIDs caused by the dynamical events such as earthquakes, Tsunamis, deep convections and volcano eruptions etc. Those are originated in the land and lower atmosphere. Finally, based on the observations and model outcomes a potential inventory parameter of MSTIDs will be proposed.

3. General approach

The general approach which will be followed in this task is presented as a block diagram as shown in Figure 1. To examine the MSTIDs climatology, at first we invade the available data resources such as TechTIDE database, CDSS and ionosonde network in Europe (Belehaki et al., 2020). Based on the necessity (if required), we also will create a new database like long-term GNSS-TEC data over the European sector.

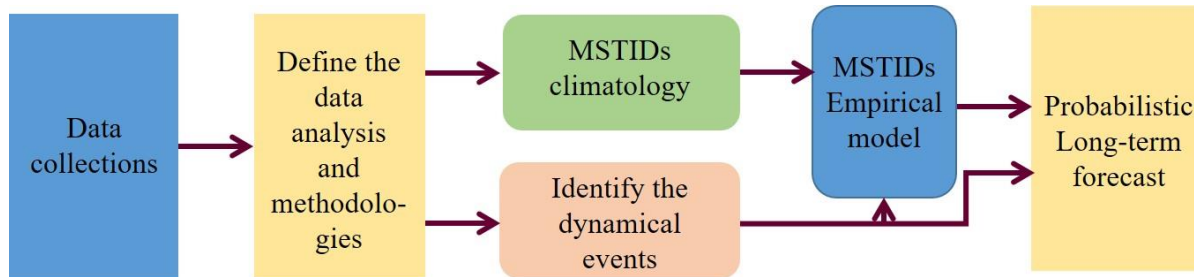


Figure 1. Block diagram of the general approach for MSTIDs climatology and probabilistic forecast.

We also revised the methodologies used in the TechTIDE project, which mainly focused on the large scale traveling Ionospheric disturbances as well as define new methodologies to establish the MSTIDs climatology using different data sets.

3.1. Data Analysis

As a first step, we looked into the TechTIDE database (<https://techtide-srv-pub.space.noa.gr/techtide/#/pages/intro>) to explore the MSTIDs climatology over Europe. However, the database is not sufficient to create the MSTIDs climatology because most of methods (except CDSS - Continuous Doppler Sounding System) used in that project was targeting to the LSTIDs. Therefore, in addition to the available datasets, we decided to develop a new database for MSTIDs climatology using the Global Navigation Satellite System-Total Electron Content (GNSS-TEC) data and ionosonde data. Moreover, the CDSS methodology is well reported in the TechTIDE project (http://techtide.space.noa.gr/?page_id=1001), we only briefly mention about them herein. Nevertheless, this is one of the potential measurements to study the MSTIDs.

Since more than 1000 GNSS-receivers data is available over the European sector and the ionosonde data is also spread across Europe, they can be used for estimation of the MSTIDs climatology, so that it can cover latitude and longitude dependency of the MSTIDs occurrence as well. The data analysis and methodologies are detailed in the section 3.2.

We have gathered the GNSS-TEC, Ionosonde and CDSS data from 2009 to 2020 and used three years of data at different solar conditions to develop the MSTIDs climatology over Europe. The detailed information about the data analysis will be presented in the next section.

3.2. Methodologies

To study the diurnal, seasonal, and solar cycle dependency of the MSTIDs occurrence and characteristics, we analyse three years of data: 2014 (solar maximum), 2016 (moderate solar activity) and 2020 (solar minimum) and for four seasons i.e. March (spring equinox), June (summer solstice), September (fall equinox) and December (winter solstice), respectively. As mentioned in the earlier section due to the wide area coverage, TEC and ionosonde data is used to explore the MSTIDs climatology. The data analysis and methodology of TEC and ionosonde data are presented in the following sections. In addition, we also use the CDSS data for investigating the dynamical events associated MSTIDs. Moreover, the swarm satellite and airglow imager data will be used to validate the forecast outcomes. A brief analysis information for all these data will be presented in sections 3.2.3, 3.2.4 and 3.2.5, respectively. Furthermore, the Northern Annular Mode (NAM) will be used to explore the source of the winter daytime MSTIDs.

3.2.1 GNSS-TEC data

The TEC maps were derived from Global Navigation Satellite system observation data in Receiver INdependent EXchange format and obtained from the regional GNSS receiver network over Europe. Maps are provided through <https://stdb2.isee.nagoya-u.ac.jp/GPS/GPS-TEC/> and a list of GNSS data providers can be found at https://stdb2.isee.nagoya-u.ac.jp/GPS/GPS-TEC/gnss_provider_list.html. The temporal and spatial resolution of the TEC data is 30 seconds and Latitude-Longitude grid of $0.25^\circ \times 0.25^\circ$.

We estimated detrended TEC (dTEC) by subtracting 1-hr running averages from the original TEC for each pair of satellites and receivers (Otsuka et al., 2013). This allowed for the investigation of TEC variations caused by MSTIDs. An example dTEC map on 02 December 2020 at 13:00 UT over Europe shown in Figure 2, which clearly represents the north-east to south-west aligned blue and red bands. In this map, vertical (horizontal) magenta (red) dotted line denotes every 5° along these lines $\pm 0.5^\circ$ averaged data is used for constructing the north-south (east-west) keograms at different longitudes (latitudes).

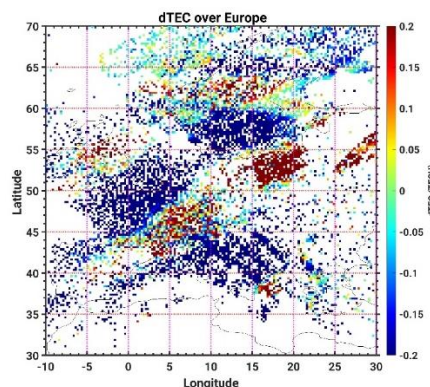


Figure 2. A sample dTEC map over Europe on 02 December 2020 at 13:00 UT.

The keogram is an effective tool to visualize the temporal and spatial evolution of the MSTIDs. Thus, it can provide more information about the MSTIDs characteristics as well as

latitude and longitude variation of MSTIDs occurrence and propagations. The EW and NS keogram of dTEC on 02 December 2020 at different latitudes and longitudes are shown in Figures 3 and 4, respectively. The EW keogram can provide information about the east or west propagation as well as EW-alignment of the MSTIDs. For example, in the present case, a periodic TEC perturbation with more than 0.2 TECU observed between 08:00 to 17:00 UT and in all the latitudes, the perturbation is progressing from west to east. On the other hand, the NS keogram provides us the information about the propagation in the north-south direction and NS-alignment of the perturbation. In figure 4, the dTEC perturbation is propagating from north to south. By combining both EW and NS keogram observation, we can conclude that on 02 December 2020, the MSTIDs are propagating towards southeast.

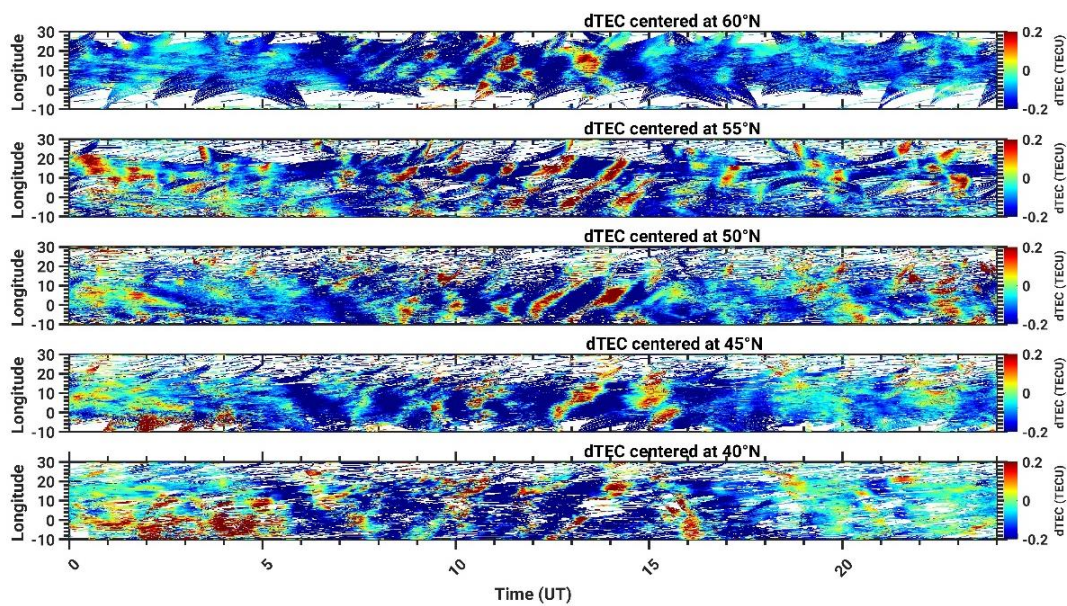


Figure 3. East-west keogram at different latitudes on 02 December 2020.

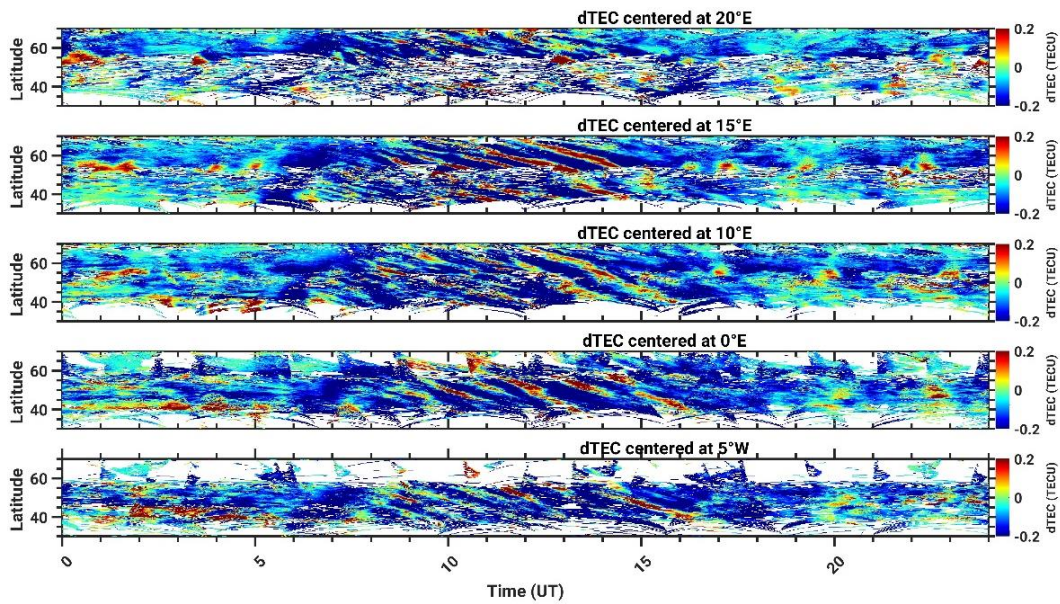


Figure 4. North-south keogram of dTEC at different longitudes over Europe on 02 December 2020.

Using the keograms, we classified eight possible propagation directions that are listed in Table 2. Through visual inspections, we identified occurrence and the direction of propagation of MSTIDs for the climatology. Furthermore, we also plan to use the fast Fourier transform (FFT) analysis to estimate the MSTIDs characteristics like, wavelength, phase speed, period and direction of propagation.

Table 2. Identification of propagation direction using the keograms

Label	Direction	Characteristics of phase front in EW and NS keogram
1	North	EWK-aligned; NSK-progression towards north
2	East	EWK-progression towards east; NSK-aligned
3	South	EWK-aligned; NSK-progression towards south
4	West	EWK-progression towards west; NSK-aligned
5	Northeast	EWK-progression towards east; NSK-progression towards north
6	Southeast	EWK-progression towards east; NSK-progression towards south
7	Southwest	EWK-progression towards west; NSK-progression towards south
8	Northwest	EWK-progression towards west; NSK-progression towards north

3.2.2 Ionosonde data

As listed in Table 1, there are 12 ionosondes of type Digisonde distributed across Europe, which are used to estimate the climatology of MSTIDs. If needed and for a slightly better geographical coverage, the ionograms of two Italian ionosondes of type Advanced Ionospheric Sounder (located in Rome and Gibilmanna) could be used optionally.

Table 1. List of ionosondes and its locations in Europe

URSI-code	Name	Latitude	Longitude	Ionosonde type
JR055	Juliusruh	54.60	13.40	DPS-4D
FF051	Fairford	51.70	358.50	DPS-4D
RL052	Chilton	51.50	359.40	DPS-1
DB049	Dourbes	50.10	4.60	DPS-4D
PQ052	Pruhonic	50.00	14.60	DPS-4D
SO148	Sopron	47.63	16-72	DPS-4D
RO041	Rome	41.90	12.50	DPS-4
EB040	Roquetes	40.80	0.50	DPS-4D
VT139	San Vito	40.60	17.80	DPS-4D
AT138	Athens	38.00	23.50	DPS-4D
EA036	El Arenosillo	37.10	353.30	DPS-4D
NI135	Nicosia	35.03	33.16	DPS-4D

Passage of traveling Ionospheric disturbances over the ionosonde locations are identified with various specific signatures in the ionograms. Some of the most familiar signatures are mid-latitude spread-F and Y/U forked structures etc. Sometimes, these different signatures are also useful to identify the plausible source of the disturbances. Therefore, we focused on the presence of six prominent structures in the ionograms for MSTIDs and sporadic-E (Es) layers, to explore their role on the nighttime MSTIDs.

We have labelled these features from one to seven for data analysis purposes as shown in Table 3. Example ionograms are depicted in Figure 5. To explore the climatology of MSTIDs we did not scale the ionograms, instead we did only the visual inspection of full hour ionograms according to the URSI Handbook of ionogram interpretation and reduction (1972).

Table 3. Catalog of TID related ionogram signatures

Label	Name/Description of ionogram signature	References
0	No ionograms	
1	Midlatitude: Frequency spreadF (FSF) $FF = f_x I - f_x F_2$ ($FF > 0.3$ MHz)	Yu et al., 2016
2	Midlatitude: Range spread (RSF)	
3	Sporadic-E (Es), $foEs > foE + 1$ MHz	Sivakandan et al., 2022
4	Y/U-forked F traces in the near of foF2	Laryunin. 2021
5	Satellite traces ST: as vertical and/or oblique traces with a slightly higher range parallel to the main 1F ionogram trace	Paul et al., 2021
6	Multi cusp signatures MCS along all traces mainly lower F region trace	Muruyama et al., 2016
7	Multi reflection echoes MRE (MRE doublet MRD)	Tsunoda, R.T., 2012.

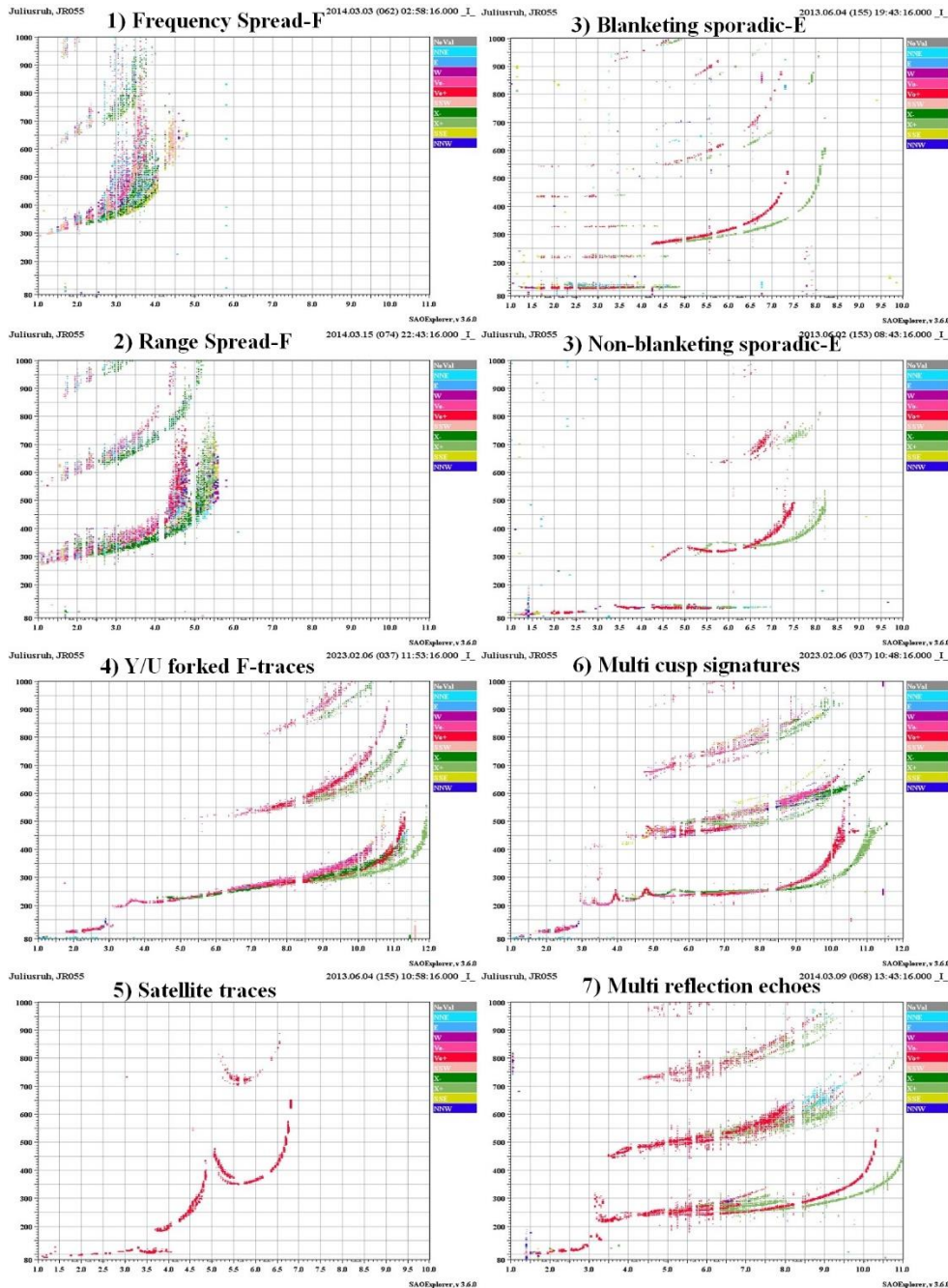


Figure 5. Potential ionogram signatures for representation of electron density variations MSTIDs activities and sporadic- E layers.

3.2.3 CDSS data

The CDSS at Czech Republic consists of five transmitters and a receiver. The frequencies of individual transmitters are shifted by 4 Hz, thus, received signals from all the transmitters can be displayed in one common Doppler shift spectrogram [Chum et al., 2010]. New CDSS installations are currently finished in Dourbes (Belgium) and Slovakia (three transmitters and one receiver each). The new data will be also available for the project needs.

The gravity waves and or MSITDs produce S-shaped patterns in the Doppler shift spectrogram that can be used to estimate the horizontal component such as wavelength, propagation direction phase velocity and period. To estimate the MSTIDs parameters during the lower atmospheric dynamical events we follow a method presented in the Figure 6 (Chum et al., 2012).

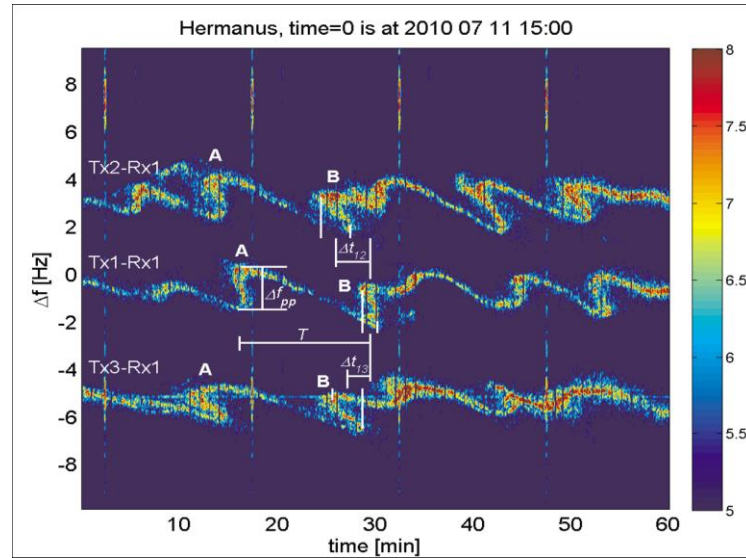


Figure 6. Tropospheric event as it was observed by South African CDSS (Hermanus site) on 11 July 2010. Transmitter-receiver paths are offset by 4 Hz. A and B indicate analyzed disturbances observed on different sounding paths. T is the observed period of GW, and Δt_{12} and Δt_{13} are the time differences between the S-shaped patterns observed on various sounding paths.

3.2.4. Airglow imager data

Similar to the dTEC maps, 630 nm airglow image data obtained from the allsky airglow imager can also provide the 2D-spatial and temporal evolution of the MSTIDs. Prior to the extraction of the MSTIDs parameters, the acquired raw images from the allsky imager should be unwarped and projected onto an equidistant grid. To further enhance the visual contrast of airglow depletions in the chosen images, we first calculated the percentage difference image/residual image (I_r). Residual images are created by picking a central image (I) and averaging it with other images taken 30 min before and after. The resulting average (I_m) is therefore an hourly running average centred on I. From there, the hourly average is subtracted from and normalized with the central image to obtain the residuals ($I_r = \frac{(I(t) - I_m)}{I_m} \times 100$). These difference/residual images were then unwarped and projected onto an equidistant grid by assuming a 630 nm peak emission altitude centred at 250 km (Sivakandan et al., 2020).

The MSTID parameters derived from image analyses. When examining an image, the distance between peaks (maxima/minima) of two-phase fronts along the phase propagation direction is considered as the wavelength. The temporal evolution of the positions of these phase fronts from a given image to the successive image provides phase velocity. Thus, the period of the MSTIDs is calculable using the horizontal wavelength and horizontal phase velocity. Few sample 630 nm residual images are shown in Figure 6 left panel.

3.2.5. Swarm satellite data

The Swarm satellites were launched on 22 November 2013 with three Low-Earth-Orbiting (LEO) spacecraft viz., Swarm-A (Alpha), -B (Bravo), and -C (Charlie). Swarm-A & -C orbit the Earth at a height of ~ 450 km in a side-by-side constellation, and Swarm-B orbits the Earth at a slightly higher altitude (~ 530 km). The three satellites are equipped with an on-board Langmuir probe to measure the plasma density and electron temperature along the satellite track. Plasma density measurements with interpolated sampling rates of 1 Hz from Swarm-A & -C could be used to study the fluctuations caused by the MSTIDs propagation. Detailed descriptions about the Swarm mission, instruments, and data can be found at <https://earth.esa.int/eogateway/missions/swarm>. An example MSTIDs signature observed in the simultaneous Swarm plasma density perturbations and in comparison with the airglow intensity and dTEC perturbation for a few nights over Northern Germany is shown in Figure 6.

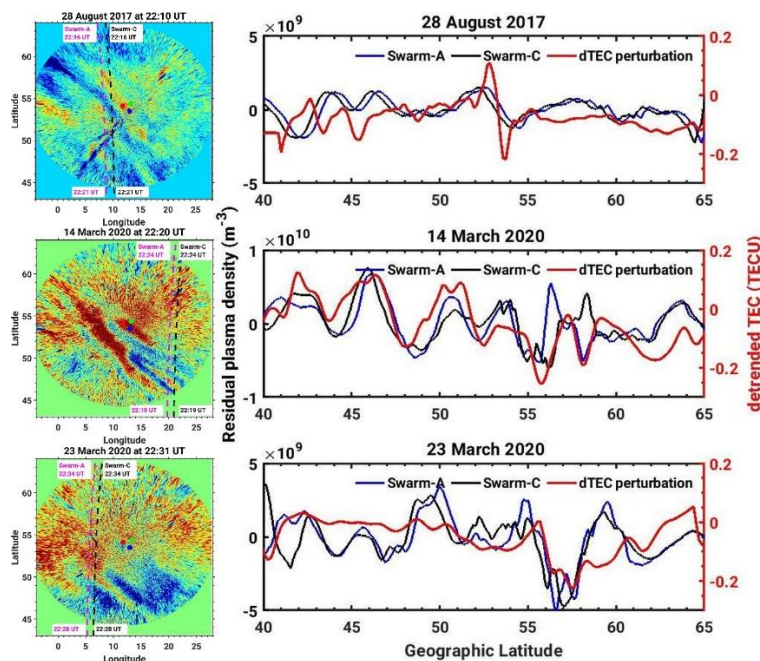


Figure 6. Left panel show the Swarm-A (magenta dotted line) & -C (black dotted line) satellites trajectory along the field of view of the airglow image with the arrival and exit time. The right panel show the Swarm-A (blue curve) & -C (black curve) measured in situ residual plasma density perturbations as well as the dTEC perturbations (from GNSS data) along the mean orbit of Swarm-A & -C on 28 August 2017 (top row), 14 and 23 March 2020 (middle and bottom row, respectively).

3.2.6. Northern Annular Mode (NAM) data

In order to explore the potential connection between the polar vortex variabilities and winter daytime MSTIDs occurrence and characteristics, we use NAM data which could be an indicator for the variabilities in the polar vortex.

The NAM (or Arctic Oscillation) is defined as the first empirical orthogonal function of northern hemisphere (20°-90°N) winter sea level pressure data. It explains 23% of the extended winter mean (December-March) variance, and it is clearly dominated by the North Atlantic Oscillations (NAO) structure in the Atlantic sector. Positive values of the NAM are associated with lower-than-normal sea level pressures over the Arctic and westerly wind anomalies along ~55°-60°N. The NAM data is available in the following link: <https://climatedataguide.ucar.edu/climate-data/hurrell-wintertime-slp-based-northern-annular-mode-nam-index>.

4. Compilation of list of dynamic events

Comprehensive observations of the effects during geomagnetic storms usually show Total Electron Content Perturbations caused by the ionospheric fluctuations associated with the neutral wind of TIDs moving equatorward. The TIDs could be multiple when associated with a series of quasi-periodic substorms (Shiokawa, et al., 2007). Severe tropospheric convection generates gravity waves throughout the full range of phase speeds, wave frequencies, and vertical and horizontal wavelengths. Horizontal wavelengths of these waves extend from approximately 10 to 1000 km, while their periods range from minutes to tens of hours (Vadas and Fritts, 2004). The most efficient meteorological source of gravity waves in mid latitudes are cold fronts (Sauli and Boaka, 2001; Lastovicka, 2006). Tropospheric sources of gravity waves further include intense thunderstorms or convective storms (Sentman, 2003; Azeem et al., 2015; Lay, 2015) and typhoons (Zuo Xiao et al., 2007; Kong et al., 2017). Extreme tropospheric events (e.g. super typhoons, hurricanes) generate Concentric TIDs (CTIDs) lasting for several hours and subsequently occurring MSTIDs, which could be detected in TEC and CDSS measurements. CTIDs are associated with concentric gravity waves (CGWs) at ionospheric heights and could exhibit horizontal phase velocities of about 100-220 m/s, horizontal wavelengths of about 160-270 km and periods of 8-30 min. During such extreme events CTIDs are excited by convective clouds, spiral rainbands and the eyewall of typhoon. There is suggested in literature that subsequent MSTIDs are generated by the electrodynamic coupling of Perkins instability and by polarization electric fields induced by CGWs (Chou, et al., 2016). During eclipse atmospheric gravity waves may be generated due to the supersonic speed of the Moon's cool shadow in the atmosphere, as theoretically has been predicted by Chimonas and Hines (1970). Such waves propagate upward with growing amplitudes and their ionospheric trace should be measurable as TIDs (Jakowski, et al., 2008).

List of the lower atmospheric dynamical events such as extratropical cyclones, deep convections, cold and warm fronts will be gathered, and the ionospheric variability during, before and after the dynamical events will be investigated. This will give the information about the

MSTIDs occurrence characteristics due to the lower atmospheric influences. Similarly, geomagnetic activity, solar eclipse, intense earthquake, tsunami and volcano eruption impact on the ionosphere and its associated MSTIDs characteristics will be examined. This will help us to understand the solar-terrestrial and lower atmosphere- ionospheric coupling processes. This information will be used to train the model to forecast the dynamical MSTIDs and alerts to these events.

References

- Azeem, I., Yue, J., Hoffmann, L., Miller, S.D., Straka, W.C., Crowley, G., (2015). Multi-sensor profiling of a concentric gravity wave event propagating from the troposphere to the ionosphere. *Geophys. Res. Lett.*, 42, p. 7874-7880. DOI: 10.1002/2015GL065903
- Belehaki, A., Tzagouri, I., Altadill, D., Blanch, E., Borries, C., Buresova, D., Chum, J., Galkin, I., Juan, J.M., Segarra, A. and Timoté, C.C. (2020). An overview of methodologies for real-time detection, characterisation and tracking of traveling ionospheric disturbances developed in the TechTIDE project. *Journal of Space Weather and Space Climate*, 10, p.42. <https://doi.org/10.1051/swsc/2020043>
- Chimonas, G., Hines, C.O., (1970). Atmospheric gravity waves induced by a solar eclipse. *Journal of Geophysical Research* 75, 875.
- Chou, M.Y., Lin, C.H., Yue, J., Tsai, H.F., Sun, Y.Y., Liu, J.Y., Chen, C.H., 2017. Concentric traveling ionosphere disturbances triggered by Super Typhoon Meranti (2016). *Geophys. Res. Lett.* <http://dx.doi.org/10.1002/2016GL072205>.
- Chum, J., T. Šindelárová, J. Lastovicka, F. Hruska, D. Buresova, J. Base: Horizontal propagation directions and velocities of Acoustic Gravity Waves in the ionosphere over the Czech Republic, *Journal of Geophysical Research*, 115, A11322, doi:10.1029/2010JA015821, 2010.
- Chum, J., R. Athieno, J. Baše, D. Burešová, F. Hruška, J. Laštovička, L. A. McKinnell, and T. Šindelárová (2012), Statistical investigation of horizontal propagation of gravity waves in the ionosphere over Europe and South Africa, *J. Geophys. Res.*, 117, A03312, doi:10.1029/2011JA017161.
- Jakowski, N, S. M. Stankov, V. Wilken, C. Borries, D. Altadill, J. Chum, D. Buresova, J. Boska, P. Sauli, F. Hruska, Lj.R. Cander, (2008). Ionospheric behaviour over Europe during the solar eclipse of 3 October 2005, *J. Solar-Terr. Phys.*, 70, 836-853.
- Kong, J., Yao, Y.B., Xu, Y.H., Kuo, C.Y., Zhang, L., Liu, L., Zhai, C.Z., (2017). A clear link connecting the troposphere and ionosphere: ionospheric responses to the 2015 Typhoon Dujuan. *JOURNAL OF GEODESY*, 91, p.1087-1097. DOI: 10.1007/s00190-017-1011-4.
- Laryunin, O. (2021). Studying characteristics of traveling ionospheric disturbances using U-shaped traces on vertical incidence ionograms, *Advances in Space Research*, 67(3), 1085-1089, <https://doi.org/10.1016/j.asr.2020.11.007>.
- Lastovicka, J., (2006). Forcing of the ionosphere by waves from below. *J. Atmos. Sol. Terr. Phys.*, 68, p. 479 – 497. DOI: 10.1016/j.jastp.2005.01.018.

- Lay, E.H., X.M., Shao, A.K., Kendrick, C.S. Carrano, (2015). Ionospheric acoustic and gravity waves associated with midlatitude thunderstorms. *J. Geophys. Res.-Space Physics*, 120, p. 6010-6020, DOI: 10.1002/2015JA021334.
- Maruyama, T., Yusupov, K., and Akchurin, A. (2016). Interpretation of deformed ionograms induced by vertical ground motion of seismic Rayleigh waves and infrasound in the thermosphere, *Ann. Geophys.*, 34, 271–278, <https://doi.org/10.5194/angeo-34-271-2016>.
- Otsuka, Y., Suzuki, K., Nakagawa, S., Nishioka, M., Shiokawa, K., and Tsugawa, T. (2013). GPS observations of medium-scale traveling ionospheric disturbances over Europe, *Ann. Geophys.*, 31, 163–172, <https://doi.org/10.5194/angeo-31-163-2013>.
- Paul, K.S., Haralambous, H., Oikonomou, C., and Paul, A. (2021). Investigation of Satellite Trace (ST) and Multi-reflected Echo (MRE) ionogram signatures and its possible correlation to nighttime spread F development from Cyprus over the solar mini-max (2009–2016), *Advances in Space Research*, 67(6), 2021, 1958-1967, <https://doi.org/10.1016/j.asr.2020.12.040>.
- Sauli, P., J. Boska, (2001). Tropospheric events and possible related gravity wave activity effects on the ionosphere. *J. Atmos. Sol. Terr. Phys.*, 63, p.945 – 950.
- Sentman, D.D., Wescott, E.M., Picard, R.H., Winick, J.R., Stenbaek-Nielsen, H.C., Dewan, E.M., Moudry, D.R., Sao Sabbas, F.T., Heavner, M.J., Morrill, J., (2003). Simultaneous observations of mesospheric gravity waves and sprites generated by a Midwestern thunderstorm. *J. Atmos.Sol.Terr. Phys.*, 65, 537 -550. DOI: 10.1016/S1364-6826(02)00328-0.
- Shiokawa, K., G. Lu, Y. Otsuka, T. Ogawa, M. Yamamoto, N. Nishitani, and N. Sato, (2007). Ground observation and AMIE-TIEGCM modelling of a storm-time traveling ionospheric disturbance, *Journal of Geophysical Research*, Vol. 112, A05308, doi:10.1029/2006JA011772.
- Sivakandan, M., Martinis, C., Otsuka, Y., Chau, J. L., Norrell, J., Mielich, J., et al. (2022). On the role of E-F region coupling in the generation of nighttime MSTIDs during summer and equinox: Case studies over northern Germany. *Journal of Geophysical Research: Space Physics*, 127, e2021JA030159. <https://doi.org/10.1029/2021JA030159>.
- Sivakandan, M., Mondal, S., Sarkhel, S., Chakrabarty, D., Sunil Krishna, M. V., Chaitanya, P. P., et al. (2020). Mid-latitude spread-F structures over the geomagnetic low-mid latitude transition region: An observational evidence. *Journal of Geophysical Research: Space Physics*, 125, e2019JA027531. <https://doi.org/10.1029/2019JA027531>.
- Yu, S., Xiao, Z., Aa, E., Hao, Y., and Zhang, D. (2016). Observational investigation of the possible correlation between medium-scale TIDs and mid-latitude spread F, *Advances in Space Research*, 58 (3), 349-357, <https://doi.org/10.1016/j.asr.2016.05.002>.
- Tsunoda, R. T. (2012). A simple model to relate ionogram signatures to large-scale wave structure, *Geophys. Res. Lett.*, 39, L18107, doi:10.1029/2012GL053179.
- Vadas, S.L., Fritts, D.C., (2004). Thermospheric responses to gravity waves arising from mesoscale convective complexes. *J. Atmos. Sol. Terr. Phys.*, 66, p.781 – 804. DOI:10.1016/j.jastp.2004.01.025.



Zuo Xiao, Sai-guan Xiao, Yong-qiang Hao, Dong-he Zhang, (2007). Morphological features of ionospheric response to typhoon. *Journal of Geophysical Research*, 112, A04304, doi:10.1029/2006JA011671., L18107, doi:10.1029/2012GL053179.